Measurement of nuclide production cross section for lead and bismuth with proton in energy range from 0.4 GeV to 3.0 GeV

Hiroki Matsuda[1,*], *Shin-ichiro* Meigo[1], *Hiroki* Iwamoto[1], and *Fujio* Maekawa[1]

[1]J-PARC/JAEA, 2-4, Shirakata, Tokai-mura, Ibaraki-ken, Japan

Abstract. For the Accelerator-Driven nuclear transmutation System (ADS), nuclide production yield estimation in a lead-bismuth target is important to manage the target. However, experimental data of nuclide production yield by spallation and high-energy fission reactions are scarce. In order to obtain the experimental data, an experiment in J-PARC using ^{nat}Pb and ^{209}Bi samples were carried out. The samples were thin foils with about 0.1 mm thick and 25 mm × 25 mm square and were irradiated with protons at kinematic energy points of 0.4 GeV, 2.2 GeV, and 3.0 GeV. After the irradiation, the nuclide production cross section was determined by spectroscopic measurement of decay gamma-rays from the samples with HPGe detectors. In this paper, 14 nuclide production cross sections for lead and bismuth were obtained. They were compared with the calculated cross sections with various models and the evaluated one.

1 Introduction

Accelerator-Driven nuclear transmutation System (ADS) transmutes minor actinides (MA) by supplying neutrons continuously. Neutrons are supplied by a spallation reaction of lead-bismuth eutectic (LBE) irradiated by 1.5 GeV energy protons, which is also utilized as coolant. For the estimation of the radioactive nuclides to treat wastes and evaluate the chemical effect of spallation products in the LBE, accurate cross section data are required. Although much effort has been devoted to conducting nuclide production cross section measurements at several facilities since the 1950s, the uncertainties of data, being typically about 10%, are not good enough to validate the calculation model. Furthermore, data around in a few GeV region, which are candidates for projectile energies of the ADS, have larger uncertainty than other regions.

Thus, the experiment was performed in J-PARC. In this experiment, lead and bismuth samples were chosen, which are employed as a structural material or the spallation target. Stacked square metal samples were placed inside a vacuum chamber in the beam dump line. They were irradiated by proton beams having different energies of 0.4 GeV, 2.2 GeV, and 3.0 GeV.

A comparison between the experimental data and the calculations were demonstrated. In this paper, the details of the experiment and analysis procedure are described.

2 Experiment

2.1 Setup

The basic experiment setup was the same as Ref. [1]. The experiment was carried out at the beam transport line from the RCS [2] to the Materials and Life Science Experimental Facility (MLF), which is called as 3NBT. Thin square foils of lead and bismuth (Goodfellow Cambridge Ltd.), 0.125 mm or 0.2 mm thick and 25 mm long, were sandwiched. Between lead and bismuth samples, thin aluminum foil (The Nilaco corporation) with 0.1 mm thick was inserted to prevent contamination of recoil nuclides. The sandwiched sample was shrouded by rectangular aluminum foils with 0.1 mm thickness and was fixed on the rectangular sample holder. Four sets of this sample were placed at the head of each linear stage guide. They were placed in the vacuum chamber that was installed in the beam dump line. A linear stage guide was controlled remotely to insert and extract samples.

2.2 Irradiation

Each sample set was irradiated by 0.4 GeV, 2.2 GeV, and 3.0 GeV protons, respectively. The 0.4 GeV beam was transported from the LINAC without acceleration. The other energies were obtained by changing the extraction timing of the kicker magnet at RCS. The beam width and position were measured with the multi-wire profile monitor (MWPM) installed in the beamline. The number of protons in the beam was monitored by the current transformer (CT). Beam profile measurement using an imaging plate (IP) was performed after irradiation to improve the accuracy of the beam position on the samples. Repetition of shots was set to 0.4 Hz to avoid melting of samples. In total, 40 shots, i.e. 2.32×10^{14} protons, were irradiated for each target.

After irradiation, the linear stage guides were removed from the chamber. Each foil was packed by the polyethylene bag with 0.1 mm thickness. The cooling time, which is the time interval between the end of the irradiation to

*e-mail: matsuda.hiroki@jaea.go.jp

the beginning of the measurement, was approximately six to nine hours.

2.3 Analysis

Decay gamma-rays from irradiated samples were measured by the high pure germanium detector (HPGe, Mirion Technologies GC2018). List of activation products analyzed in this paper was summarized in table 1.

Table 1. The list of nuclides

Nuclide	Half-life	The main gamma-ray keV (Absolute intensity %)
^{7}Be	53.22 d	477.6(10.44)
^{22}Na	2.6018 y	1274.537(99.940)
^{85}Sr	64.849 d	514.001(96)
^{127}Xe	36.346 d	202.860(68.7)
^{139}Ce	137.63 d	165.8575(79.90)
^{169}Yb	32.018 d	177.213(22.28)
^{183}Re	70.0 d	162.330(25.1)

The samples were mounted on the acrylic spacer apart from the head of HPGe by about 5 cm or 25 cm to keep detector-to-sample geometry rigidly. The production cross section of specified nuclei σ was written as

$$\sigma = \frac{C}{t_l \epsilon I_\gamma \mu} \times \frac{t_r}{1 - \exp(-\lambda t_r)} \times \frac{\exp(\lambda t_c)}{N_p n} \quad (1)$$

where C is the number of count of a peak, t_l is so-called live-time which includes deadtime correction during measurement, ϵ is the efficiency at the peak energy, I_γ is the absolute gamma-ray intensity, μ is the self-absorption correction, t_r is so-called real-time, λ is the decay constant of the nuclide, N_p is the number of protons irradiated, and n is the number density of the sample. Here the correction during irradiation was not applied since the irradiation time was considerably shorter than the half-life of products.

The recoil particles could be trapped by the forward and backward aluminum foils. It was negligibly small according to a calculation. However, they were observed in the actual aluminum foil. The activity of them was evaluated as a negligible amount. Thus, this correction was not applied in this experiment.

The effects of secondary particles affecting the backward samples were also estimated by the simulation. Since very thin samples were employed in this experiment, the number of secondary particles was lower than the irradiated protons in the order of three or four digits. Hence, this effect was not considered in this analysis.

The number density of the sample n is derived by

$$n = \frac{m}{MS} N_{\mathrm{A}} \quad (2)$$

where m is the sample mass that is measured by the electric scale, S is the surface area of the sample, M is the atomic weight of the sample, and N_{A} is Avogadro constant.

The self-absorption correction μ is calculated by

$$\mu = \frac{1 - \exp(\mu_{\mathrm{att}} \rho t)}{\mu_{\mathrm{att}} \rho t} \quad (3)$$

where μ_{att} is the attenuation coefficient, ρ is the sample density, and t is the thickness of the sample. Detector efficiency of the HPGe was evaluated by using ^{241}Am, ^{152}Eu, and ^{60}Co, ^{137}Ce standard gamma-ray sources, which were put at the same position as the samples. Sum-peak corrections for multi gamma-ray sources were applied [3].

The number of protons and beam profile (width and position) were measured precisely by the CT and the MWPM, respectively. Beam profile measurement using an imaging plate (FUJI-FILM BAS-SR2040) was also performed to improve the accuracy of the beam profile. The irradiated samples were placed onto the IP to expose. After exposure, the IP was scanned by the image processor (GE healthcare Typhoon FLA 7000). Scanned images were fit by a two-dimensional Gaussian to evaluate the width and position of the beam. Here the Gaussian shape was guaranteed by the measurement of the MWPM. Finally, the fractions of the proton beam on the sample foils were derived by integrating the function over the sample area. As a result, the fractions ranged from 0.98 to 1.00. This fraction was used for the final correction of the cross section determination.

The sample surface area was measured by a typical image scanner (EPSON GT-S650). The samples were scanned with 800 dots/inch to make a binary image. The number of dots in the sample area was multiplied by a conversion coefficient.

2.4 Uncertainty estimation

The list of uncertainties concerned is shown in table 2. The uncertainty of the detector efficiency was the standard deviation of differences between measured points and calculated ones. Imaging plate uncertainty, namely the uncertainty of irradiated proton fraction, was evaluated as the standard deviation of proton fraction of all samples at the same energy.

The reading uncertainty of scanning of 1 mm scale with 800 dots/inch, i.e., 314.96 dots/mm, was 1 dot. In addition, an ambiguity for an edge detection could be estimated as 2 dots. Thus, the uncertainty of the sample surface was evaluated as 1.4 % by a square root of the sum of the square of 3/314.96.

Table 2. Table of uncertainties

Description	Estimated uncertainty %
Statistics of gamma-ray count	<0.1–10
Detector efficiency	1.3
Sample weight	<0.1
Sample surface area	1.4
Time	<0.1
Self-absorption	0.1
The number of proton	3
Imaging plate	<0.1
Branching ratio	<30
In total	3.6–31.8

3 Results and discussion

The PHITS code [4] was employed to calculate the production cross sections with two intranuclear cascade models (Bertini and INCL4.6 [5]) and two generalized evaporation models (GEM and Original-GEM (denoted as Gen.GEM in plots) developed by Furihata [6]). The calculation by using INCL++ code [7] with INCL++v6.0.1 and ABLA07 [8] models was also performed. The number of histories was sufficiently large so that calculation uncertainties were negligible. In Fig. 1 and Fig. 2, the measured, the calculated, and the evaluated cross sections of JENDL-HE/2007 [9] for each production cross sections of lead and bismuth were shown. The other experimental data were taken from EXFOR [10–21].

The mean square deviation factor $\langle F \rangle$ [22] was usually employed as the quantitative scale for comparisons between the experimental data and the calculated one. The $\langle F \rangle$ and its standard deviation S ($\langle F \rangle$) are derived as

$$\log_{10}(\langle F \rangle) = \sqrt{\left\langle \log_{10}\left(\frac{\sigma_{\mathrm{cal}}}{\sigma_{\mathrm{exp}}}\right)^2 \right\rangle} \tag{4}$$

$$S\,(\langle F \rangle) = \left\langle \left[\log_{10}\left(\frac{\sigma_{\mathrm{cal}}}{\sigma_{\mathrm{exp}}}\right) - \log_{10}\langle F \rangle \right]^2 \right\rangle \tag{5}$$

where $\sigma_{\mathrm{exp}}(\sigma_{\mathrm{cal}})$ is the experimental (calculated) cross section, and $\langle\ \rangle$ means averaging over the all points in comparison between J-PARC experiment and calculations. If there were no difference between the experiment and the calculation, $\langle F \rangle$ would become zero. The $\langle F \rangle$ for each target are summarized in table 3.

Table 3. The $\langle F \rangle$ of each calculation for lead and bismuth

	$\langle F \rangle \pm S\,(\langle F \rangle)$	
Calculation model	Lead	Bismuth
Bertini/GEM	3.16 ± 0.58	10.37 ± 2.87
Bertini/Gen.GEM	2.19 ± 0.27	11.39 ± 3.03
INCL4.6/GEM	6.40 ± 2.00	14.97 ± 4.08
INCL4.6/Gen.GEM	5.09 ± 1.53	14.27 ± 3.79
INCL++v6.0.1/ABLA07	1.88 ± 0.16	3.74 ± 0.72
JENDL/HE-2007	3.19 ± 0.59	4.55 ± 0.87

This clearly showed that the INCL++ code agrees well for lead in the all calculations since it was developed taking into account the GSI measurement [23, 24]. However, it was not in bismuth case, though there is one proton difference between lead and bismuth. Considering all the experimental data, including J-PARC, the JENDL data had lower peak energy at the local maximum of cross section than other calculations, which appeared nuclides heavier than xenon for both samples. This reason might come from a utilization of Jet AA Microscopic Transport Model (JAM) [25] model for the evaluation of the data above 250 MeV.

By using the Original-GEM, the calculations agreed with the experimental data except for Bertini model at the bismuth sample. The main difference between GEM and original-GEM was a treatment of a Coulomb potential calculation. The Coulomb potential in GEM was adjusted to a slightly lower value than one in Original-GEM, which made more particles evaporating at an excited state, resulting in the lower yield for spallation products.

4 Summary

The production cross sections from lead and bismuth with 0.4 GeV, 2.2 GeV, and 3.0 GeV protons were measured at J-PARC. In total, 14 cross sections were obtained with higher accuracy than other experimental data in the past thanks to quite stable J-PARC beam and monitoring systems. The present results were compared with the calculations and the evaluated nuclear data. The present experimental data suggested that further improvement of models is mandatory in the GeV energy region. The evaluated data was in good agreement with the experimental data in some energy points. However, function shapes differed from the experimental data and the calculations.

Acknowledgement

The authors are grateful to Mrs. Nishikawa and Hirano, and the members of Nippon Advanced Technology (NAT) for technical assistance with the experiments and to Drs. Saha, Hotchi, and Harada for tuning of the RCS.

References

[1] H. Matsuda, S. Meigo, H. Iwamoto, J. Nucl. Sci. Technol. **3131**, 1 (2018)
[2] S. Meigo, F. Noda, S. Ishikura, et al., Nucl. Instruments Methods Phys. Res. Sect. A Accel. Spectrometers, Detect. Assoc. Equip. **562**, 569 (2006)
[3] E. Tomarchio, S. Rizzo, Radiat. Phys. Chem. **80**, 318 (2011)
[4] T. Sato, Y. Iwamoto, S. Hashimoto, et al., J. Nucl. Sci. Technol. **3131**, 1 (2018)
[5] A. Boudard, J. Cugnon, J.C. David, et al., Phys. Rev. C **87**, 014606 (2013)
[6] S. Furihata, Nucl. Instruments Methods Phys. Res. Sect. B Beam Interact. with Mater. Atoms **171**, 251 (2000), 0003036
[7] D. Mancusi, A. Boudard, J. Cugnon, et al., Phys. Rev. C **90**, 054602 (2014), arXiv:1407.7755v2
[8] A. Kelic, M.V. Ricciardi, K.H. Schmidt (2009), 0906.4193
[9] Y. Watanabe, K. Kosako, S. Kunieda, et al., J. Korean Phys. Soc. **59**, 1040 (2011)
[10] V. Zerkin, B. Pritychenko, Nucl. Instruments Methods Phys. Res. Sect. A Accel. Spectrometers, Detect. Assoc. Equip. **888**, 31 (2018)
[11] R. Michel, M. Gloris, J. Protoschill, et al., J. Nucl. Sci. Technol. **39**, 242 (2002)
[12] M. Gloris, R. Michel, F. Sudbrock, et al., Nucl. Instruments Methods Phys. Res. Sect. A Accel. Spectrometers, Detect. Assoc. Equip. **463**, 593 (2001)
[13] Y.E. Titarenko, V.F. Batyaev, V.M. Zhivun, et al., Pramana **68**, 289 (2007)

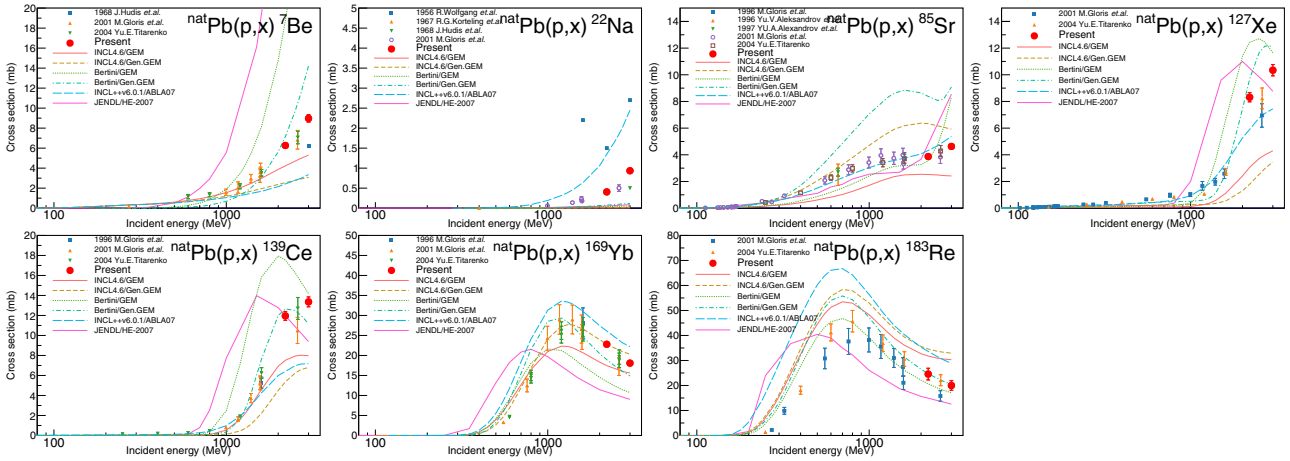

Figure 1. Production cross sections of ^{7}Be, ^{22}Na, ^{85}Sr, ^{127}Xe, ^{139}Ce, ^{169}Yb, and ^{183}Re from ^{nat}Pb. This works (full circle), other experiments (other symbols) taken from EXFOR, calculations (solid and dashed lines), and the evaluated data (bold line) are plotted.

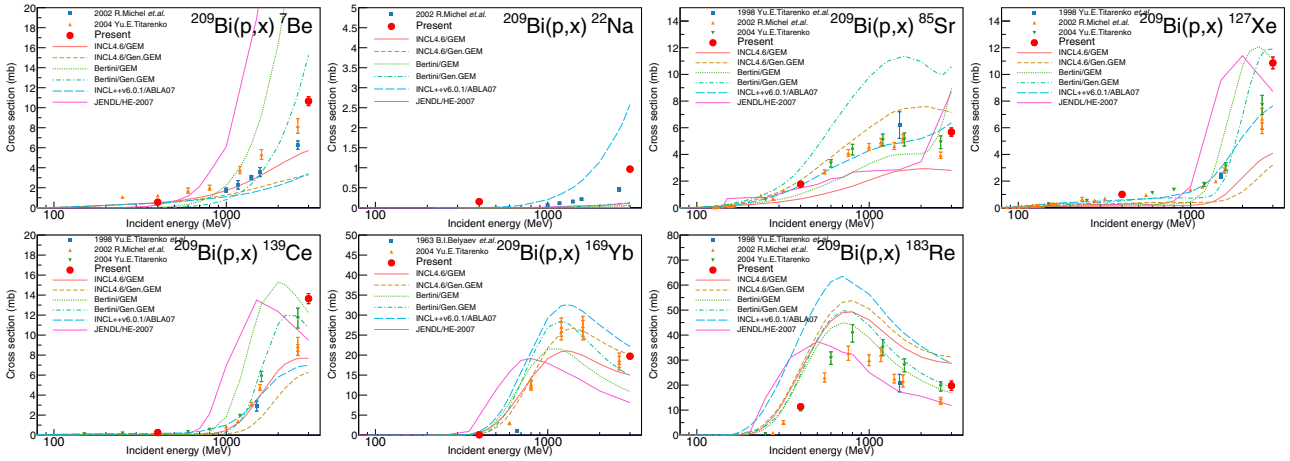

Figure 2. Production cross sections of ^{7}Be, ^{22}Na, ^{85}Sr, ^{127}Xe, ^{139}Ce, ^{169}Yb, and ^{183}Re from ^{209}Bi. This works (full circle), other experiments (other symbols) taken from EXFOR, calculations (solid and dashed lines), and the evaluated data (bold line) are plotted.

[14] Y.V. Alexandrov, V.P. Eismont, R.B. Ivanov, et al., *Cross section for the production of radionuclides in lead target irradiated with 660 MeV protons* (Uppsala Univ, Sweden, 1997), ISBN 91-506-1220-4

[15] Y. Titarenko, O. Shvedov, M. Igumnov, et al., Nucl. Instruments Methods Phys. Res. Sect. A Accel. Spectrometers, Detect. Assoc. Equip. **414**, 73 (1998)

[16] M. Gloris, R. Michel, U. Herpers, et al., Nucl. Instruments Methods Phys. Res. Sect. B Beam Interact. with Mater. Atoms **113**, 429 (1996)

[17] R. Wolfgang, E.W. Baker, A.A. Caretto, et al., Phys. Rev. **103**, 394 (1956)

[18] Y.V. Alexandrov, V.P. Eismont, R.B. Ivanov, et al., *New Data for the Production of Radionuclides in Thin Lead Target by 660 MeV Protons*, in *Proc.Intern.on Nucl. Data Sci. Technol.* (1997)

[19] J. Hudis, S. Tanaka, Phys. Rev. **171**, 1297 (1968)

[20] R.G. Korteling, A. Caretto, J. Inorg. Nucl. Chem. **29**, 2863 (1967)

[21] B. Belyaev, A. Kalyamin, A. Murin, Bull.Russian Acad. Sci. - Phys. **27**, 907 (1963)

[22] Y.E. Titarenko, O.V. Shvedov, V.F. Batyaev, et al., Phys. Rev. C **65**, 064610 (2002)

[23] T. Enqvist, W. Wlazło, P. Armbruster, et al., Nucl. Phys. A **686**, 481 (2001)

[24] B. Fernández-Domínguez, P. Armbruster, L. Audouin, et al., Nucl. Phys. A **747**, 227 (2005)

[25] Y. Nara, N. Otuka, A. Ohnishi, et al., Phys. Rev. C **61**, 024901 (1999), 9904059